Effects of layer structure of the skin on the measured signal by optical coherence tomography

Wanrong Gao (高万荣), Maohai Hu (胡茂海), Qian Chen (陈 钱), Xin Yue (悦 鑫), Qi Jiang (蒋 琪), Peng Li (李 鹏), Jianhui Fu (符建辉), Jingli Zhu (朱景丽), Xiaochun Yang (杨晓春), and Lianfa Bo (柏连发)

Optical Engineering Department, Nanjing University of Science and Technology, Nanjing 210094

Optical coherence tomography (OCT) is a noninvasive cross-sectional imaging modality capable of measuring tissue morphology and function with high spatial resolution. Both the amplitude and the phase of the interometric heterodyne signal can be exploited to obtain the profile of sample reflectivity related to its microstructure and the bi-directional blood flowing velocity information. The fact that the skin and human mucosa have a layer structure suggests that the backscattered signal from tissue arises from two sources. The first is the scattering particles within the tissue. The second is the Fresnel refraction on the interface between two layers. However, the analysis available only considers one aspect of the backscattering sources. In this paper, we report an analysis that is based on the combination of both the particle scattering within the tissue and the Fresnel reflection on the interfaces between two layers. The new model is more reasonable for establishing the relationship between the signal detected by OCT scanner and tissue structures.

OCIS codes: 170.3340, 170.4500, 230.4170, 170.3660.

Optical coherence tomography (OCT)[1−3] is a noninvasive cross-sectional imaging modality based on measuring the backscattering properties of tissue to determine physiological state. The development of the rapid-scanning optical delay (RSOD) lines and real-time data-processing techniques make it possible to produce *in vivo* cross-sectional images of tissue[4]. For *in vivo* scattering-based tissue diagnosis imaging, the important potential sources of scattering are the organelles of cells and the extracellular medium, each of which has an index different from their surroundings. These include nucleus, mitochondria, lysosomes, peroxisomes, and connective tissue fibers (bundles of elastin and collagon)[5,6]. Investigations show that the overall shape of the nucleus influences small-angle scattering whereas the effects of small intracellular organelles are more evident at higher angles. At the same time, comparing the scattering pattern of collagen with that of a cell, the likelihood of high-angle scattering events is markedly increased for fibrous tissue components such as collagen[5]. This phenomenon is important for *in vivo* OCT applications in the detection of dysplasia in epithelial tissues. Because OCT detects the backscattered light, it is possible that collagen could dominate scattering from cells when the volume of interrogation includes a layer of cells lying on top of a layer of collagen. Dysplastic changes originate near the basal layer and propagate upword. Scattering from the reticular fibers in the basal layer and underlying stroma might override more subtle scattering changes caused by nuclear abnormalities and mitotic activity in mildly dysplastic cells[5].

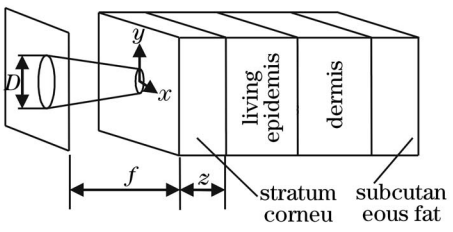

Fig. 1. Schematic of the sample arm geometry of the OCT scanner.

Human skin has a layered structure consisting of discrete homogeneous regions of scattering particles. It is derived from two embryological layers. The epidermis is formed from the ectoderm, and the deeper layer of the skin is formed from the mesoderm[7]. Adult skin is a dynamic tissue; the outer layer of the epidermis forms the stratum corneum; cornified dead cells are in the process of being sloughed off. The second layer of the human skin is the living epidermis which contains primarily living cells. In order to analyze positions of the vessels and consider the effects of the blood flowing on the measured signal, the dermis is sub-divided into the layers according to the geometry and sort of the blood vessels distribution within the skin[7]. The first dermal layer is the papillary dermis which contains capillary loops generally orientated perpendicularly to the surface of the skin capillary loops. These superficial capillary loops with the inner diameter about 2–40 μm are perfused by low-speed red blood cells that supply the tissue with oxygen and nutritive substances and remove waste metabolites. The arterioles, venules and arterio-venous anastomosises with inner diameter of 10–40 μm which take an active part in body temperature regulation are located under the upper blood net dermis (80-μm thickness). Reticular dermis includes small arteries and veins (20–60 μm inner diameter) mainly orientated perpendicularly to the surface of the skin. These small vessels constitute routs for blood supply and drainage to veins and arteries (50–100 μm inner diameter) from the deep blood net dermis and subcutaneous fat. The model structure of the human skin is shown in Fig. 1. The values of the refractive index n_s, the scattering coefficient μ_s, the backscattering cross section μ_b, scattering anisotropy factor g and the thickness t_s of each layer of the human skin are given in Table 1.

The layer structure of the human skin and the existence

Table 1. Refractive Index and Optical Coefficients of Human Skin Tissues[8,9]

Skin Layer	μ_s (mm^{-1})	μ_b (mm^{-1})	g	n_s	Thickness (μm)
Stratum Corneum	100	0.069	0.9	1.53	20
Living Epidermis	40	0.069	0.85	1.34	80
Papillary Dermis	30	1.8	0.8	1.4	250
Upper Blood Net Dermis	35	1.8	0.9	1.39	80
Reticular Dermis	20		0.76	1.4	1500
Deep Papillary Net Dermis	35		0.95	1.39	170
Subcutaneous Fat	15		0.8	1.44	6000

of backscattering centers such as collagen and microtubules suggest that both the Fresnel reflection between two tissue layers and backscattering from small tissue components (for example, the collagen and microtubules) contribute to the detected OCT signal. The effect of backscattering signal component has been omitted in the previous theoretical models[10,11]. In this paper, we will combine these two signal components to give a more reasonable signal formula.

The mean square heterodyne signal current $\langle i^2(z)\rangle_r$ of the OCT system produced by the reflection from the inter-surface between two layers can be expressed by[12,13]

$$\langle i^2(z)\rangle_r = \frac{4\alpha^2 P_r P_s R_d}{k^2\omega_H^2}\left[\exp(-2\mu_s z) + \frac{2\exp(-\mu_s z)\left[1-\exp(-\mu_s z)\right]}{1+\omega_s^2/\omega_H^2} + \left[1-\exp(-\mu_s z)\right]^2\frac{\omega_H^2}{\omega_s^2}\right], \quad (1)$$

where ω_H and ω_s are the $1/e$ irradiance radii in the detected plane in the absence and presence of scattering and are given by $\omega_H^2 = (f/kD)^2$ and $\omega_H^2/\omega_s^2 = 1\Big/\left\{1+\left[2D/\rho_0(z)\right]^2\right\}$. D is the $1/e$ intensity radius of reference and sample beams in the lens plane. The quantity $\rho_0(z)$ is the lateral coherence length of the reflected sample field in the mixing plane and is given by $\rho_0(z) = \sqrt{3/\mu_s z}\,(\lambda/\pi\theta_{rms})\left[1+nd(z)/z\right]$, and $d(z) = f-(z/n_s)$. α is the conversion factor for power to current. P_r and P_s are the powers of the reference and the input sample beams, respectively. ω_0 is the $1/e$ intensity radius of these beams in the lens plane. R_d is the Fresnel reflection coeffient. The first term within the brackets of Eq. (1) represents the contribution due to the single scattering. The third term is the multiple-scattering effect and the second term is the cross term. The advantage of Eq. (1) is that it includes the so-called shower curtain effect[14].

The mean-squared heterodyne-signal current $\langle i^2(z)\rangle_s$ at the detector contributed by the scatterers within the source coherence length L_c, defined by $L_c = \int_{-\infty}^{\infty}|\gamma(\tau)|^2 d\tau$, can be expressed as[15]

$$\langle i^2(z)\rangle_s = \frac{\alpha^2 P_r P_s}{4}\frac{\mu_b \pi D^2 L_c \exp(-2\mu_s z)}{2(n_s z+f)^2\left\{1+\left[\frac{n_s z\pi D^2}{4\lambda_0 f(n_s z+f)}\right]^2\right\}}, \quad (2)$$

where μ_b is the backscattering coefficient of the sample, which is defined as $\mu_b = \eta\sigma_b$. η is the number density of the particles ($1/\mu m^2$), σ_b (μm^2) is the backscattering cross section of a particle. The total mean-squared heterodyne-signal current $\langle i^2(z)\rangle_t$ is then given by

$$\langle i^2(z)\rangle_t = \langle i^2(z)\rangle_r + \langle i^2(z)\rangle_s . \quad (3)$$

In OCT, the illumination and collecting are realized using a lens with an numerical aperture (NA) less than 0.5[16]. Therefore, we can use the normal incident approximation to find the reflectance R and transmittance T[17]:

$$R = \left(\frac{n_t - n_i}{n_t + n_i}\right)^2, \qquad T = \frac{4n_t n_i}{(n_t+n_i)^2}, \quad (4)$$

here the n_i and n_t are the index of refraction for the incident medium and transmitting medium, respectively. As shown in Fig. 2, if the index of refraction of the surrounding medium is n_0, the index of refraction of the stratum corneum is n_1, the living epidermis n_2, the papillary dermis n_3, the upper blood net dermis n_4, reticular dermis n_5, the reflectance R_i for the each interface can be calculated with the following Eq. (6). The reflected power from each interface is then given by

$$R_0 P_s,\ T_1^2 R_1 P_s,\ T_2^2 T_1^2 R_2 P_s,\ \cdots, \quad (5)$$

where R_0, R_1, R_2 are the reflectance at the surface, first interface and second interface, respectively. T_1 and T_2 are

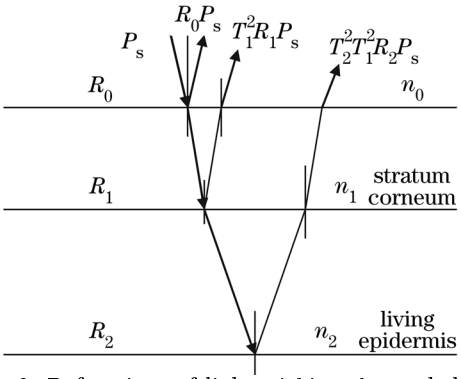

Fig. 2. Refractions of light within a layered skin.

the transmittances at first interface and second interface, respectively. Equation (5) shows that when probing the refractive index discontinuities within the tissue, the reflected power from a specific interface is determined by both the refractive index discontinuities at the point and the refractive index discontinuities above it. This fact suggests that interpreting the OCT signal and evaluating the maximum probing depth of an OCT scanner, it is necessary to account the effect of the refractive index discontinuities above an interested point. Based on this consideration, the power of the input sample beam $P_{\rm s}$ should be replaced by the effective sample power $P_{\rm eff}$. For each interface, the effective sample power $P_{\rm eff}$ is defined as

$$P_{\rm eff1} = T_1^2 R_1 P_{\rm s},\ P_{\rm eff2} = T_2^2 T_1^2 R_2 P_{\rm s},\ \ldots\ldots\ . \qquad (6)$$

The layer structure of the human skin requires that the sample power $P_{\rm s}$ in Eqs. (1) and (2) should be replaced by the effective power $P_{\rm eff}$ given by Eqs. (6). Because the Eqs. (3) contains both the Fresnel reflection between two tissue layers and backscattering from small tissue components such as moving blood cells, it permits the calculation of tissue structure information as well as the velocity of the moving cells by means of coherent detection and short-time Fourier transform[2]. At the same time, as is shown previously, the maximum imaging depth within the human skin can be obtained for OCT scanner based on the use of Eqs. (3) and (6). We believe that this imaging depth is more reasonable because it accounts effects of the differences of refraction index between two layers and the backscattering contribution of the tissue elements.

Assume that the OCT system is with shot-noise limited detection, the mean square noise power N is given by[15] $N = 2\alpha q G^2 R_{\rm l} P_{\rm r} B_{\rm w}$, where R_1 is the resistance of the load, G is gain of the amplifier, and $\rm B_w$ is the system bandwidth. The maximum imaging depth is determined by the minimum detectable signal-to-noise ratio. As is done by Thrane et al[15], if 3 is used as the minimum detectable SNR, we obtain the formula for the maximum imaging depth $z_{\rm m}$,

$$[\langle i^2(z_{\rm m})\rangle_{\rm r} + \langle i^2(z_{\rm m})\rangle_{\rm s}]/N = 3\ . \qquad (7)$$

In conclusion, OCT technique makes it possible to obtain the *in vivo* optical cross-section images of skin to help the diagnosis of skin disorders. Based on the analysis of the scattering properties of the tissue components and the layer structure of the skin, we obtain one formula for the signal in OCT scanner. The advantages of this model are that because it accounts both the Fresnel reflection between two tissue layers and backscattering from small tissue components, it may be used to calculate the possible detected OCT signal as well as the maximum imaging depth with good accuracy.

This work was supported by the Key Lab Foundation of The Modern Optical Technology of Jiangsu Province, Soochow University (No. KJS01002), the Young Foundation of Nanjing University of Science and Technology (No. Njust200302), the Natural Science Foundation of Jiangsu Province (No. BK2004133), and the Foundation for Returned Scholars of Personal Ministry of China (No. KZ04001). W. Gao's e-mail address is gaowangrong@yahoo.com.

References

1. I. D. Huang, E. A. Swanson, C. P. Lin, J. S. Schuman, W. G. Stinson, W. Chang, M. R. Hee, T. Flotte, K. Gregory, C. A. Puliafito, and J. G. Fujimoto, Science **248,** 1178 (1991).
2. J. A. Izatt, M. D. Kulkarai, S. Yazdanfar, J. K. Barton, and A. J. Welch, Opt. Lett. **22,** 1439 (1997).
3. S. Yazdanfar, "Noninvasive microstructural and velocity imaging in humans by color Doppler optical coherence tomography", Ph. D. Dissertation, Case Western Reserve University (2003).
4. G. J. Tearney, B. E. Bouma, and J. G. Fujimoto, Opt. Lett. **22,** 1811 (1997).
5. R. Drezek, A. Dunn, and R. Richards-Kortum, Appl. Opt. **38,** 3651 (1999).
6. J. M. Schmitt and G. Kumar, Appl. Opt. **37**, 2788 (1998).
7. I. V. Meglinsky and S. J. Matcher, Proc. SPIE **3915,** 18 (2000).
8. J. M. Schmitt, A. Knüttel, and R. F. Bonner, Appl. Opt. **32,** 6032 (1993).
9. J. A. Izatt, M. R. Hee, G. M. Owen, E. A. Swanson, and J. G. Fujimoto, Opt. Lett. **19,** 590 (1994).
10. J. M. Schmitt, and A. Knüttel, J. Opt. Soc. Am. A **14,** 1231 (1997).
11. L. Thrane, H. T. Yura, and P. E. Andersen, J. Opt. Soc. Am. A **17,** 484 (2000).
12. L. Thrane, H. T. Yura, and P. E. Andersen, Proc. SPIE **3915,** 2 (2000).
13. L. Thrane, H. T. Yura, and P. E. Andersen, J. Opt. Soc. Am. A **17,** 484 (2000).
14. I. Dror, A. Sandrov, and N. S. Kopeika, Appl. Opt. **37,** 6495 (1998).
15. L. Thrane, H. T. Yura, and P. E. Andersen, Proc. SPIE **3915,** 2 (2000).
16. J. M. Schmitt, IEEE J. Sel. Top. Quantum Electron. **5,** 1205 (1999).
17. E. Hecht, *Optics* (Addison Wesley, San Francisco, 2002) chap.4.